

THE ELECTRIC POTENTIAL DISTRIBUTION IN THE DISTURBED POLAR IONOSPHERE: COMPARISON OF STATISTICAL MODELS WITH THE DATA OF SELECTED SUBSTORM INTERVALS

S.B. Lunyushkin¹, O.I. Bergardt¹, V.V. Mishin¹, V.M. Mishin¹, D.Sh. Shirapov²

¹*Institute of Solar-Terrestrial Physics SB RAS, Irkutsk, Russia, e-mail: lunyushkin@iszf.irk.ru*

²*East Siberia State University of Technology and Management, Ulan-Ude, Russia*

Abstract. Large-scale maps of the electric potential distribution in the disturbed polar ionosphere during the relatively weak 26 February 2008 substorm obtained by two different methods, are compared with each other. One series of the electric potential maps has been derived on the basis of SuperDARN measurement data, another set maps has been calculated by the magnetogram inversion technique. We also compare graphs of variation of the cross polar cap potential drop during the considered substorm, obtained by the two methods. The SuperDARN maps are founded to mainly describe the regular, whereas the MIT maps – both regular and irregular components of the spatial electric potential distribution.

Introduction

Electric fields and currents in the high-latitude regions of the Earth's ionosphere are the most important components of the coupled magnetosphere-ionosphere (M-I) system. These ionospheric electric fields and currents are largely driven by magnetospheric electric fields and currents, which are in turn driven by interactions between the magnetosphere and the solar wind. These interactions occur via reconnection between the interplanetary magnetic field (IMF) and the dayside geomagnetic field and by means of the quasi-viscous mechanism in magnetospheric boundary layers. Based on the dependence of high-latitude electric fields on the IMF and solar wind parameters or geomagnetic conditions, a number of statistical or empirical models of large-scale electric potential distributions in the polar ionosphere has been derived from the measurement data by the DMSP and DE-2 satellites and SuperDARN radars [Papitashvili and Rich, 2002; Ruohoniemi and Greenwald, 2005; Weimer, 2005; Cousins and Shepherd, 2010].

Along with the well-known system of large-scale plasma convection vortices and electric currents in the M-I system, researchers have become aware of formation of mesoscale cells during substorms, each of which involves a plasma vortex and a field-aligned current (FAC) [Kauristie et al., 2000; Shi et al., 2012; Mishin et al., 2013]. Also, in recent years, studies of the mesoscale and large-scale variability in the high-latitude ionospheric convection have been initiated on the basis of the SuperDARN measurement data [Cousins et al., 2013].

In this paper, we analyze the observed dynamics of the electric potential distributions in the polar ionosphere from the data on the 26 February 2008 substorms. The time series of the electric potential distributions (2D maps) were calculated by using the magnetogram inversion technique (MIT-ISTP) [Mishin et al., 1979; Mishin, 1990; Mishin et al., 2000]. These MIT data calculated for the specified instants are compared with the similar data obtained from statistical results of measurements with SuperDARN radars.

Data

We use the above MIT, the results of measuring the plasma and IMF parameters onboard spacecraft WIND (<http://omniweb.gsfc.nasa.gov>), the AE indices that we obtained from 42 ground-based magnetic stations at the geomagnetic latitudes $\Phi > 40^\circ$, and the above statistical model for the electric potential distribution in the ionosphere derived from SuperDARN measurement data (<http://vt.superdarn.org/tiki-index.php>). The MIT input data are three components of the variable magnetic field vector measured by the network comprising 110 ground-based magnetometers in the northern hemisphere at $\Phi > 40^\circ$ (see references in Acknowledgements). The main MIT output data are: three types of 2D distribution maps of the equivalent ionospheric current density, the electric potential (U), the FAC density, and Joule heating power released in the polar ionosphere (Q_i). The maps are calculated each minute on a fixed grid with grid size $M_{Lat} \times M_{Long} = 1^\circ \times 10^\circ$. On the basis of 2D distribution maps of the FAC density, the polar cap boundary is determined as the R1 high-latitude boundary, by which we calculate the open magnetic flux (Ψ_1) through the polar cap and the Poynting flux into the magnetosphere, $\epsilon' = \text{const} \cdot (\Psi_1)^2 \cdot V_{SW}$ [Mishin et al., 1992; Mishin et al., 2000]. We use our own spatially inhomogeneous and variable in time model for the corpuscular electric conductivities of the polar ionosphere [Shirapov et al., 2000].

Fig. 1b shows that during the addressed 02–06 UT interval of the 26 February 2008 events, the solar wind dynamic pressure (P_d) varies with a small amplitude around the mean, comparatively low and quasi-constant, 1.5 nPa level. The pre-onset phase of the first observed disturbance cycle is initiated near 02:45 UT by the IMF B_z southward turn up to the ~ -1.5 nT level (Fig. 1a). The AE index (Fig. 1c) growth starts near 02:50 UT from an extremely low level < 10 nT. Further, one observes a slow, almost monotonous, growth in AE to an increased, but

still low level of ~ 22 nT. Similar peculiarities are noted in the other substorm seen on the AE plot. Such low AE levels are a rare peculiarity of the addressed events. Nevertheless, Fig. 1e exhibits the signatures of two substorms' EOs (expansion onsets) that are observed within (04:05–04:07) and (04:52–05:00) UT intervals, respectively, which does not contradict the research results of the 26 February 2008 events previously published in [Angelopoulos *et al.*, 2008; Pu *et al.*, 2010]. Fig. 1e illustrates the coincidence of the above EOs with the starts of fast and deep drop of the open magnetic flux (Ψ_1) in the magnetotail. One can see two Ψ_1 growth phases, i.e. two phases of the magnetic flux and energy accumulation (necessary substorm signatures), on the Ψ_1 plots in both addressed substorms. The Ψ_1 growth phase in the second substorm is superimposed onto the first substorm expansion phase continuation and recovery phase. Fig. 1f shows variations in the input Poynting flux ε' and in the substorm power Q released during the substorm. We discuss these variations below.

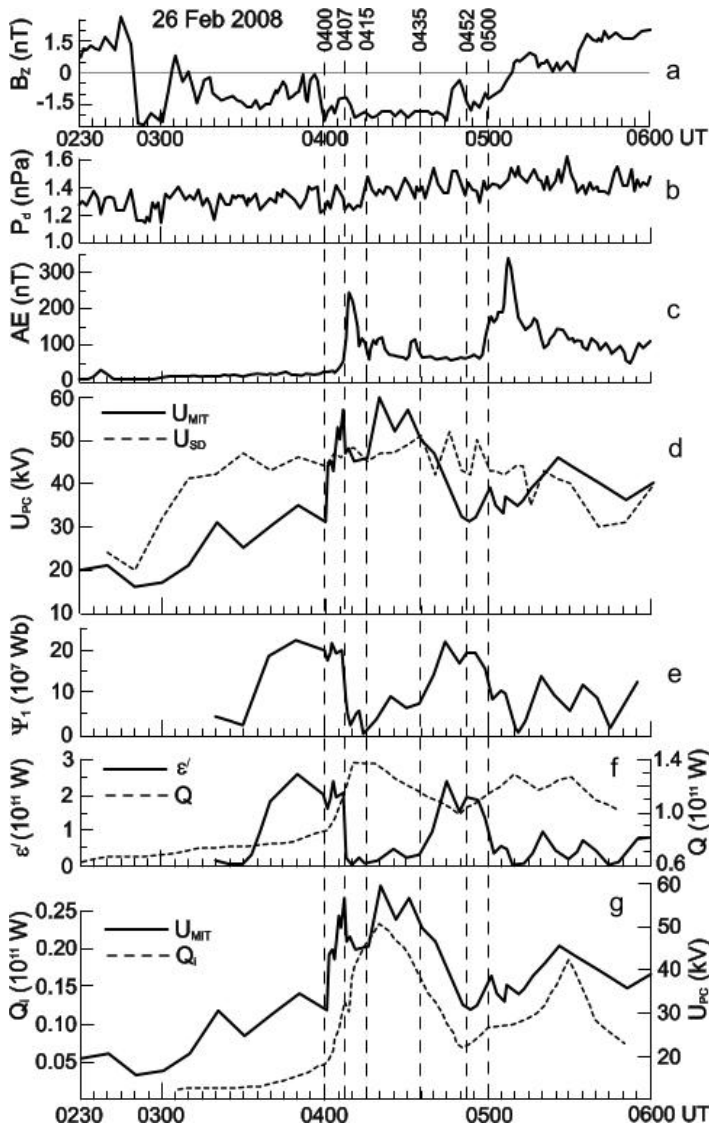


Figure 1. 26 Feb 2008 events, variations of solar wind and main energetic parameters. (a) IMF B_z component, (b) solar wind pressure P_d , (c) AE-index, (d) two plots of the polar cap potential drop U_{PC} , (e) variable open lobe magnetic flux Ψ_1 , (f) Pointing flux from solar wind into magnetosphere ε' and the total substorm power Q , (g) the plots of U_{PC} and the polar ionosphere Joule heating power Q_i .

In general, both events feature a short duration, low P_d level, and extremely low values of power Q and AE index. The latter is observed constantly except a small interval near the AE maximum. In fact, we deal with a scarcely studied type of mini-substorms with the power $Q \leq 1 \cdot 10^{11}$ W (Fig. 1f). Despite the AE low values ($AE < 300$ nT), from variation plots of basic parameters, Ψ_1 , input power ε' , and the maximal substorm power Q , we define the addressed events as ordinary small substorms [Petrukovich *et al.*, 2000].

Results

We compare the MIT-calculated U potential distributions with their analogs based on the statistical data of the direct SuperDARN measurements. Fig. 2 shows two examples of the comparison of such maps on the 26 February 2008 events: the first (at 04:06 UT) corresponds to the end of the growth phase, and the second (at 04:30 UT) – to the stable substorm regime. Under quiet (disturbed) conditions, it is usually taken that the U -isolines form a system of convection with two large-scale vortices of the DP2 (DP1) type. In fact, the distributions close to such a pattern is seen in Fig. 2d at 04:30 UT. However, the convection system at 04:06 UT (Fig. 2c) mismatches the expected pattern. In this case, the contributions of mesoscale and large-scale vortices are visually comparable, or mesoscale vortices even predominate. The arrows on the SuperDARN maps (Figs. 2a and 2b) indicate the ionospheric wind velocities. Their directions and the plasma convection velocity directions on the MIT maps (Figs. 2c and 2d) should approximately coincide. In fact, one can clearly see convection mesoscale vortices in the domains of the real SuperDARN measurements. These vortices are spatially close to those on the MIT maps. However, the known DP-2 and DP-1 large-scale convection vortices dominate on the SuperDARN maps, whereas additional convection vortices are obvious on the MIT maps. One can see a significant contribution of plasma mesoscale vortices to the general system of the ionospheric plasma convection.

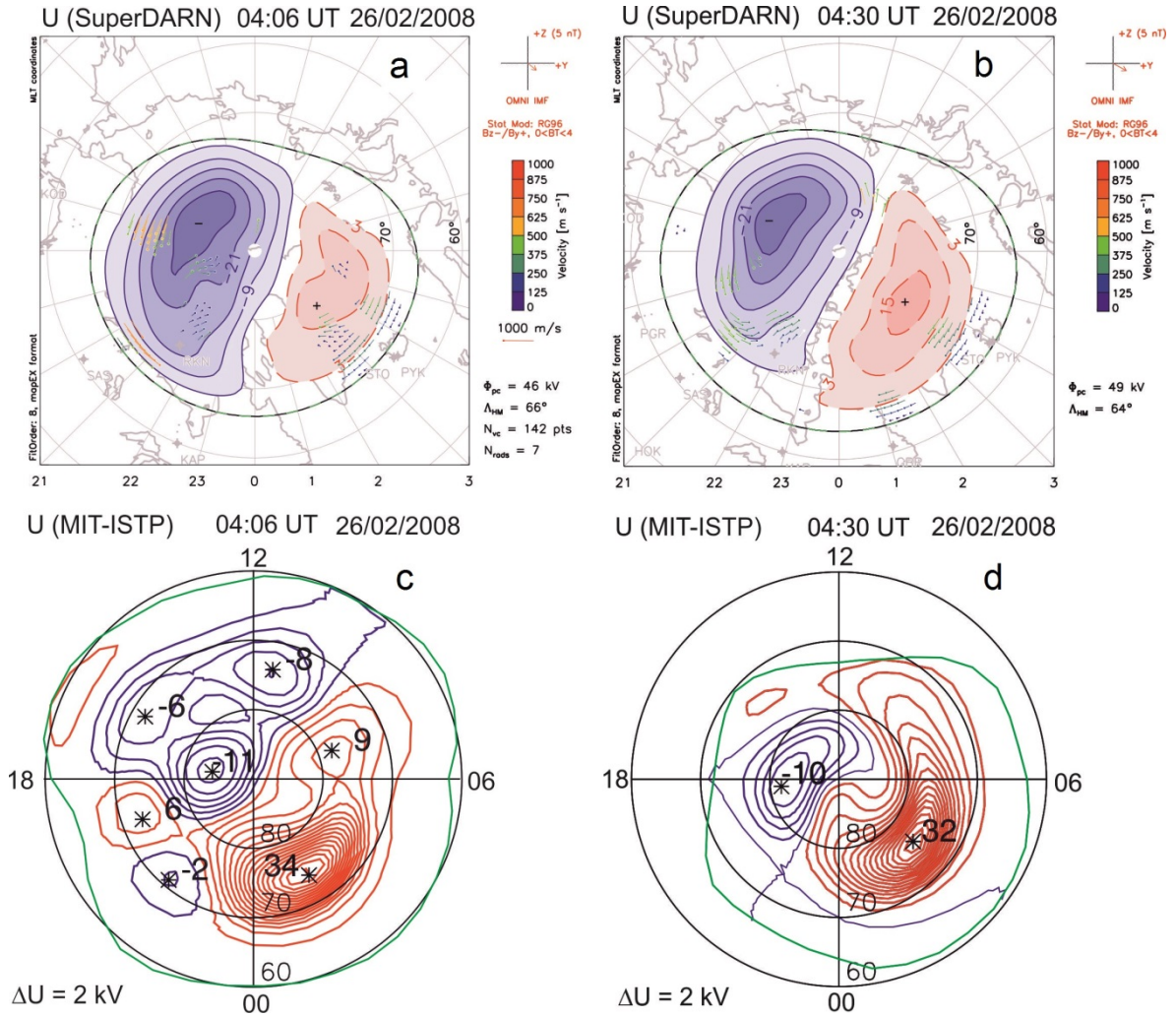


Figure 2. 26 Feb 2008, comparison of maps of distribution in polar ionosphere for wind velocities and electric potentials. Two examples are shown from the SuperDARN data (top) and MIT data (bottom). Isolines with a positive (negative) value are for the counterclockwise (clockwise) plasma vortices.

Fig. 1d presents additional examples, the plots of the U_{PC} potential extremal value difference from the MIT data and its analog from the SuperDARN data. Based on these data, we make two conclusions: (1) the mesoscale cell system increases the U_{PC} maximal values, and (2) mesoscale cells superpose two comparatively short-time pulses with U maxima on the U growth long-time pulses near 04:30 and 05:30 UT, respectively. The long-term pulse correlates with the variations in IMF B_z , short pulses are the effect of the inner mechanism that generates two substorms based on the first pulse. The short pulses are shown in Fig. 1g, where there are the plots of U_{PC} and of the polar ionosphere Joule heating power Q_i .

In general, the addressed two types of the electric potential distributions describe two different components of spatial distribution of termed parameters: the regular component from the SuperDARN data, and the irregular one from the ground-based magnetometer and MIT data. The latter corresponds to substorms, and dominates in mesoscale cells. The maps for these two types do not contradict, but supplement each other.

Conclusions

In this paper, we compared the maps of the electric potential distributions, obtained by two different methods: on the basis of MIT and by measurements of the SuperDARN radars.

The main difference between these two methods is that the radars provide direct measurements in real time in only a few areas available to each of the radars. On the remaining area of each map, the values of the electric potential are obtained by averaging of multiyear measurements and spatial extrapolation of these average values. These operations do not hampering the measure of the regular component, but they smooth out the irregular component of the ionospheric plasma drift velocity, which may play a major role during substorms.

In contrast, the ground-based magnetometer network allows us to obtain the electric potential map for a specified time without averaging, these results, in turn, contain their own error of the MIT method.

The main findings of this study are as follows.

1. Both methods give the expected and qualitatively similar large-scale, two-vortex systems of the ionospheric convection with similar values of the cross polar cap potential drop, $U_{PC} \sim (42-46)$ kV.
2. The method, based on SuperDARN measurements data, cannot detect the irregular component in the electric potential distributions, whereas the MIT method reflects the development of the corresponding mesoscale convection vortices during substorms. Even for the considered weak substorm the irregular component of about 20 kV is observed, which is comparable to the contribution of the regular component.

Apparently, the two above methods could be an important addition to each other.

Acknowledgments. We thank the ISTP SB RAS MIT group members for the assistance in the calculations. The AE index was obtained through the Website of the World Data Center for Geomagnetism, Kyoto. We are grateful to PIs of the CANOPUS, INTERMAGNET, GIMA, MACCS, IMAGE and SuperDARN international projects and of magnetic networks in Arctic and the Antarctic (the Shafer Institute of Cosmo-Physical Research and Aeronomy SB RAS, Arctic and Antarctic Research Institute, and DMI), and individual magnetic observatories for providing magnetic data used in this study. SL, VVM and VMM are supported by the Russian Foundation for Basic Research under Grants 14-05-91165 and 15-05-05561; OB is supported by FSR program No.II.12.2.3.

References

- Angelopoulos, V., et al. (2008), Tail reconnection triggering substorm onset, *Science*, 321(5891), 931-935, doi:10.1126/science.1160495.
- Cousins, E. D. P., and S. G. Shepherd (2010), A dynamical model of high-latitude convection derived from SuperDARN plasma drift measurements, *J. Geophys. Res.*, 115(A12), A12329, doi:10.1029/2010ja016017.
- Cousins, E. D. P., T. Matsuo, and A. D. Richmond (2013), Mesoscale and large-scale variability in high-latitude ionospheric convection: Dominant modes and spatial/temporal coherence, *J. Geophys. Res. Space Physics*, 118(12), 7895-7904, doi:10.1002/2013JA019319.
- Kauristie, K., V. A. Sergeev, M. Kubyshkina, T. I. Pulkkinen, V. Angelopoulos, T. Phan, R. P. Lin, and J. A. Slavin (2000), Ionospheric current signatures of transient plasma sheet flows, *J. Geophys. Res.*, 105(A5), 10677-10690, doi:10.1029/1999ja900487.
- Mishin, V. M., A. D. Bazarzhapov, and G. B. Shpynev (1979), Electric Fields and Currents in the Earth's Magnetosphere, in *Dynamics of the Magnetosphere*, edited by S. I. Akasofu, pp. 249-268, Springer Netherlands, doi:10.1007/978-94-009-9519-2_12.
- Mishin, V. M. (1990), The magnetogram inversion technique and some applications, *Space Sci Rev*, 53(1), 83-163, doi:10.1007/bf00217429.
- Mishin, V. M., A. D. Bazarzhapov, T. I. Saifudinova, S. B. Lunyushkin, D. S. Shirapov, J. Woch, L. Eliasson, H. Opgenoorth, and J. S. Murphree (1992), Different Methods to Determine the Polar Cap Area, *J. Geomag. Geoelectr.*, 44(12), 1207-1214, doi:10.5636/jgg.44.1207.
- Mishin, V. M., C. T. Russell, T. I. Saifudinova, and A. D. Bazarzhapov (2000), Study of weak substorms observed during December 8, 1990, Geospace Environment Modeling campaign: Timing of different types of substorm onsets, *J. Geophys. Res.*, 105(A10), 23263-23276, doi:10.1029/1999ja900495.
- Mishin, V. M., Z. Pu, V. V. Mishin, and S. B. Lunyushkin (2013), Short-circuit in the magnetosphere-ionosphere electric circuit, *Geomagnetism and Aeronomy*, 53(6), 809-811, doi:10.1134/s001679321306008x.
- Papitashvili, V. O., and F. J. Rich (2002), High-latitude ionospheric convection models derived from Defense Meteorological Satellite Program ion drift observations and parameterized by the interplanetary magnetic field strength and direction, *J. Geophys. Res.*, 107(A8), 1198, doi:10.1029/2001ja000264.
- Petrukovich, A. A., W. Baumjohann, R. Nakamura, T. Mukai, and O. A. Troshichev (2000), Small substorms: Solar wind input and magnetotail dynamics, *J. Geophys. Res.*, 105(A9), 21109-21117, doi:10.1029/2000ja900057.
- Pu, Z. Y., et al. (2010), THEMIS observations of substorms on 26 February 2008 initiated by magnetotail reconnection, *J. Geophys. Res.*, 115(A2), A02212, doi:10.1029/2009ja014217.
- Ruohoniemi, J. M., and R. A. Greenwald (2005), Dependencies of high-latitude plasma convection: Consideration of interplanetary magnetic field, seasonal, and universal time factors in statistical patterns, *J. Geophys. Res.*, 110(A9), A09204, doi:10.1029/2004ja010815.
- Shi, Y., E. Zesta, L. R. Lyons, J. Yang, A. Boudouridis, Y. S. Ge, J. M. Ruohoniemi, and S. Mende (2012), Two-dimensional ionospheric flow pattern associated with auroral streamers, *J. Geophys. Res.*, 117(A2), A02208, doi:10.1029/2011ja017110.
- Shirapov, D. S., V. M. Mishin, A. D. Bazarzhapov, and T. I. Saifudinova (2000), Adapted dynamic model of ionospheric conductivity, *Geomagnetism and Aeronomy*, 40(4), 471-475.
- Weimer, D. R. (2005), Improved ionospheric electrodynamic models and application to calculating Joule heating rates, *J. Geophys. Res.*, 110, A05306, doi:10.1029/2004ja010884.